Petroleum & Coal
ISSN 1337-7027

Available online at www.vurup.sk/petroleum-coal
Petroleum & Coal 57(3) 246-252, 2015

EXPERIMENTAL AND COMPUTATIONAL FAILURE ANALYSIS OF FLOW EROSION ON NEW THROTTLE IN GAS DRILLING

Yukun Fu [1], Juan Wang [2]

[1] Gas Production Engineering Research Institute, Southwest Oil & Gas Field Company, Petro China, Guanghan 618300, China; [2] Downhole Service Company, ChuanQing Drilling Engineering Company Limited, CNPC, Chengdu 610051, China

Received March 26, 2015, Accepted June 4, 2015

Abstract

Erosion wear is one of the main failure styles for wedge core in gas drilling. Mathematic model of turbulent and erosion wear for new throttle were established based on the combined technologies of fluid dynamics and erosion theory. Using this model, the distributions of maximum erosion on wedge core at different openings and the changing law of maximum erosion rate at different openings, different velocities and different diameters of particles were investigated. Final, the simulation results were validated with the field experiment results. The results show the maximum erosion rate increases with inlet velocity increasing. The erosion rate decreases with increasing particle diameters at the range of 0.6 mm to 2 mm. The erosion rate was the largest at the minimum opening. The maximum erosion rate was found on the top and end of the wedge core surface, which was entirely consistent with the experiment results. The optimization of the top and end of the wedge core and the selection of material with better anti-erosion performance can reduce the erosion damage of wedge core.

Keywords: gas drilling; wedge core; erosion wear; impinging; failure analysis.

1. Introduction

The gas drilling technology is rapidly developed in China [1-3]. As the important throttle equipment of wellhead manifold, the performances of throttle become the key to ensure the normal drilling. As the gas-solid two-phase flow velocity is huge, solid particle erosion wear has become the one of the important reasons for the flow parts failure in gas drilling. A wide variety of methods were adopted to study the erosion wear of throttle, including erosion of theoretical analysis [4-5], model derivation [6-7], computer simulation [9-12], prediction [13-15] and relevant experiments [16-18]. However, most of the researches on the wedge throttle were limited to flow field analysis and structural optimization [19-22], the erosion of failure analysis and test is relatively fewer.

Present study was concerned with the wedge core of high-pressure throttle. Mathematic model of turbulent and erosion wear for high-pressure throttle were established based on the combined technologies of computational fluid dynamics and erosion theory. Then this model was applied to study the changing law of maximum erosion rate at different openings, different velocities and different diameters of particles, and the maximum erosion places at different openings. The simulation results were validated with field experiment results so as to put forward some improvements and references for the follow-up improving design.

2. The geometric model of wedge throttle

The wedge-shaped throttle with wedge core and seat is commonly used in Tarim Oilfield of China. It can regulate the wellhead flow velocity well and avoid much more vibration damage for its low vibration. The wedge core is greatly eroded by a large amount of cutting particles contained in the fluid during the process of gas drilling. Fig. 1 shows the shape of wedge core, and Fig. 2 shows the inner flow field model of wedge throttle.

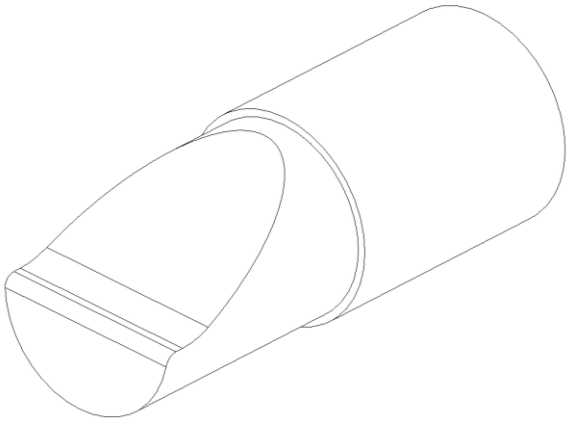

Fig. 1. 3D view of wedge core

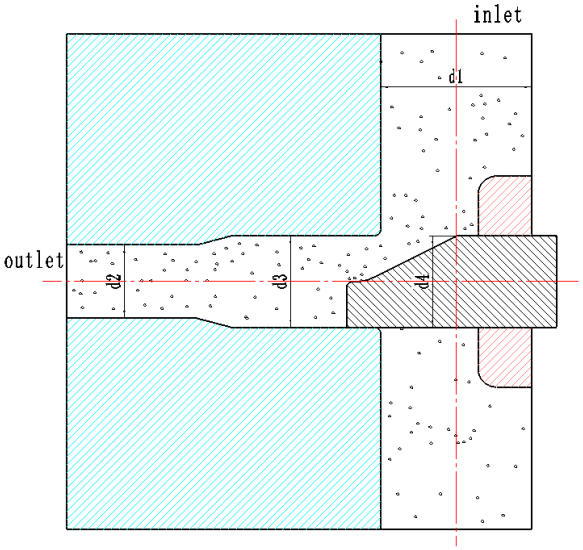

Fig. 2. The inner flow field model of wedge throttle

3. The mathematical model of particle erosion rate

3.1 Governing equations

Navier-Stokes equation for two phase flow is used to describe the fluid dynamics, considering the gas volume fraction and the effect of gas-particle resistance [8, 17].

Continuity equation

$$\frac{\partial}{\partial t}\left(\phi_g \rho_g\right)+\nabla\bullet\left(\phi_g \rho_g v_g\right)=0 \tag{1}$$

Momentum equation

$$\frac{\partial}{\partial t}\left(\phi_g \rho_g v_g\right)+\nabla\bullet\left(\phi_g \rho_g v_g v_g\right)=-\phi_g \nabla p+\nabla\bullet\left(\phi_g \tau_g\right)+\phi_g \rho_g g-f_{dr} \tag{2}$$

$$\phi_g=1-\sum_1^l V_i/\nabla V \tag{3}$$

$$f_{dr}=\frac{1}{\nabla V}\sum_1^l F_{dr,i} \tag{4}$$

3.2. Collision model and kinematic equation of solid particle

3.2.1 Hard-sphere model of discrete particle

The inter-particle collision is described by hard-sphere model of discrete particle [8], and Fig. 3 shows the collision diagram of solid phase particle. The hard-sphere model, which is based on the Quasi Binary instantaneous collision and neglects the particles deformation during collision process, shows high calculation efficiency.

For non-slip collision, the average speeds and angular velocities are listed as:

$$v_{p1}=v_{p1}^0+\left[\left(1+e\right)\left(\vec{n}\bullet\overrightarrow{G^0}\right)\vec{n}+\frac{2}{7}\left|G_{ct}^0\right|\vec{t}\right]\frac{m_2}{m_1+m_2} \tag{5}$$

$$v_{p2}=v_{p2}^0+\left[\left(1+e\right)\left(\vec{n}\bullet\overrightarrow{G^0}\right)\vec{n}+\frac{2}{7}\left|G_{ct}^0\right|\vec{t}\right]\frac{m_1}{m_1+m_2} \tag{6}$$

$$\omega_{p1}=\omega_{p1}^0-\frac{5}{7R_1}\left|\overrightarrow{G_{ct}^0}\right|\left(\vec{n}\times\vec{t}\right)\frac{m_2}{m_1+m_2} \tag{7}$$

$$\omega_{p2} = \omega_{p2}^{0} - \frac{5}{7R_2}\left|\overrightarrow{G_{ct}^{0}}\right|\left(\vec{n}\times\vec{t}\right)\frac{m_1}{m_1+m_2} \tag{8}$$

Superscript 0 represent the component before collision, subscript 1, 2 represent particle 1 and 2 respectively.

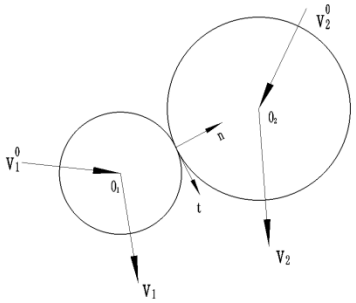

Fig. 3 Collision diagram of solid phase particle.

3.2.2 Kinematic equation of solid phase

Equation (9) is used to describe the kinematic behavior of solid phase [4-5]:

$$\frac{dv_p}{dt} = \frac{3C_D\rho_g}{4\rho_p d_p}\left(v_g - v_p\right)\left|v_g - v_p\right| + \left(1-\frac{\rho_g}{\rho_p}\right)g_z + F_z \tag{9}$$

3.3. Erosion wear model of throttle surface

According to the gas-solid two phase flow characteristics during gas drilling and taking into full consideration of the collision velocities, collision angles, shapes and mass flow, the models of Grant and Tabakoff are used for this simulation [12]:

$$E = \left|1+k_2k_{12}\sin\left(\frac{\gamma}{\gamma_0}\bullet\frac{\pi}{2}\right)\right|^2 \bullet \left|\frac{v_p}{v_1}\right|^2 \cos^2\gamma\left(1-R_T{}^2\right) + \left|\frac{v_p}{v_2}\sin\gamma\right|^4 \tag{10}$$

$$R_T = 1-\frac{v_p}{v_3}\sin\gamma \tag{11}$$

4. Simulation results and analysis

4.1 Effect of different velocities at the maximum erosion rate

The erosion rate changes with the change of inlet velocity. Fig. 4 shows the simulation results and fitting curves of the throttle erosion wear rate with different inlet velocities when the diameter of the solid particle is 0.001m, mass flow is 0.4 kg/s, and the valve opening is 50%. Clearly, the result indicates that the erosion rate in the internal valve body of the wedge is increasing with the inlet velocity increasing. The erosion damage tends to be serious along with the increase of the inlet velocity in gas drilling.

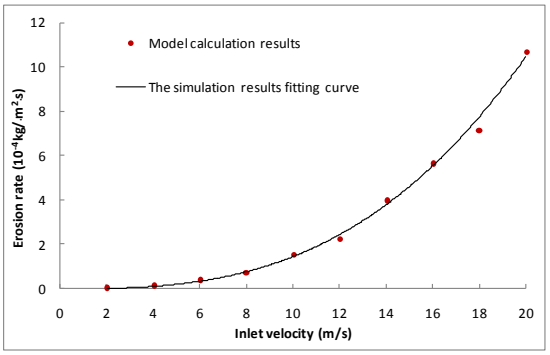

Fig. 4 The relationship between the maximum erosion rate and the inlet velocity.

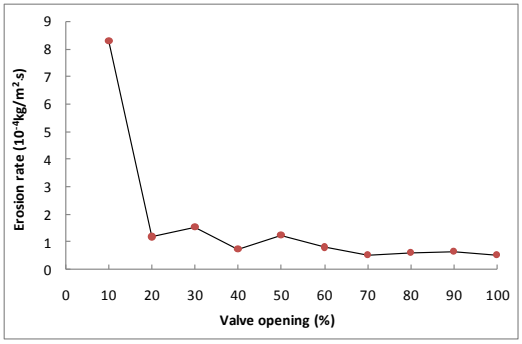

Fig. 5 The relationship between maximum erosion rate and opening

4.2 Effect of different openings at the maximum erosion rate

The erosion rate is changing during the closure process of wedge throttle. Fig. 5 shows the maximum erosion wear rate of internal valve body is inversely proportion to the valve opening. The erosion rates at the opening of 60%-90% changes little, and the average rate is 0.6×10^{-4}kg/ (m^2.s). The erosion rate reaches the maximum at the opening of 10%, 8.27×10^{-4}kg/ (m^2.s), which is 13.7 times of the maximum opening. The result indicates that the erosion rate in the internal valve body of the wedge has a serious tendency with the opening reducing during the closure process.

4.3 Effect of particle diameters on the maximum erosion rate

When the solid particle is collision in the internal of the new type of throttle valve, the maximum erosion rate with the particles of different diameter varies. Fig. 6 shows that at the range of 0.6~2 mm, the maximum erosion rate decreases along with the increase of the diameter of the solid particle at the same flow velocity. It indicates that the solid particles with larger diameters are more easily collided, increase the contact area, and decrease the pressure on the throttle surface and the erosion rate finally.

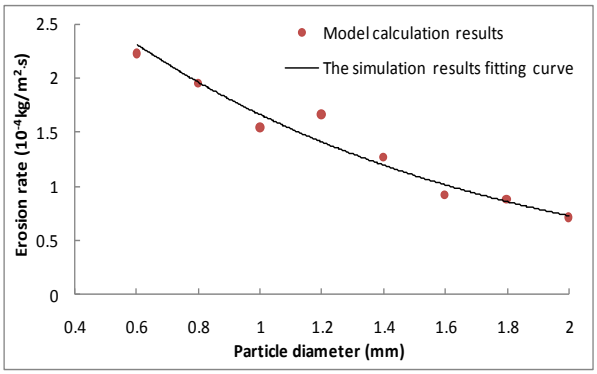

Fig. 6. The relationship between the maximum erosion rate and the diameter of particles

Fig. 7. The field experiment of erosion

5. Experimental

In order to prove the feasibility of simulation model, we did experiment on the erosion of the wedge throttle after suspending the air flow in real situation, observed the position of erosion on wedge core, and compared the position with that in simulate results.

5.1 Equipments and methods

Wedge throttle is provided by Chongqing Xintai Mechanical Limited Liability Company in China. The material of wedge core is YG8, its chemical compositions and mechanical properties are shown in Table 1 and Table 2 [3].

Table 1 Chemical composition of YG8 sample *(wt%)*

Sample	WC (wt %)	Al_2O_3 (wt %)	Co (wt %)	VC (wt %)	Re (wt %)
YG8	92.0	0	8	0	0

Table 2 Mechanical properties of YG8 sample

Sample Code	Density ($g\cdot cm^{-3}$)	Microhardness (MPa)	Bending strength (MPa)	Impact toughness ($kg\cdot m\cdot cm^{-2}$)
YG8	14.88	89.0	1493	0.25

The erosion experiment of wedge throttle was carried out in Tarim Oil Field in China. The gas medium was air, and the particles purity was greater or equal to 99.9%. The particle diameters varied from 0.8 mm to 1 mm. The pressure of experiment was 35 MPa, and the experiment lasted for 80 hours. Fig. 7 shows the equipments of field erosion experiment.

5.2 Comparative analysis

In order to understand the local erosion rate on wedge core, the main face of the wedge core was divided into 60 pieces along axial. Fig. 8(a) shows the max corrosion rate at different opening. Clearly, the maximum erosion rate was found on the top and end of the wedge core surface, which is 3 to 4 times larger than on the middle of the wedge core surface. Erosion damage will occur on the top and the end of the wedge core surface after a long-term use.

Fig. 8(b) shows the erosion of wedge core after 80 hours at the pressure of 35 MPa. Clearly, the main erosion of wedge core was found on the top and end of the wedge core surface, which was entirely consistent with the model result. The accuracy of the simulation results was verified.

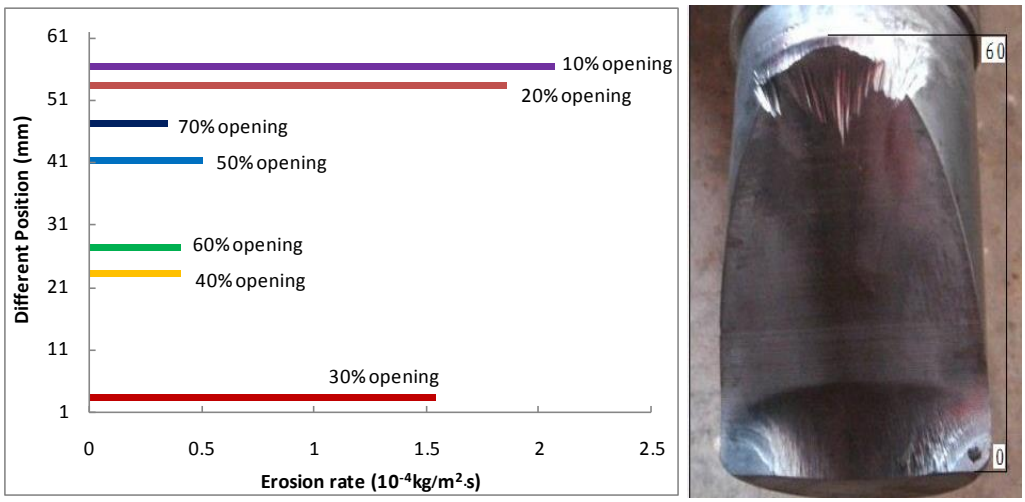

Fig. 8 The comparison of maximum erosion zones from simulation and experiment results.

6. Conclusions

(1) The maximum erosion rate increases with inlet velocity increasing. The erosion rate decreases with the increase of particle diameter at the range of 0.6mm to 2mm. The erosion rate was largest at the minimum opening.

(2) The maximum erosion rate was found on the top and end of the wedge core surface. The experiment result was entirely consistent with the simulation result, which verifies the accuracy of the simulation model.

(3) According to the erosion position of wedge core, the optimization of the top and end of the wedge core is the next working focus. Selecting material with better anti-erosion performance can also reduce the erosion damage of wedge core.

Nomenclature

ρ_g	*The gas density (kg/m^3)*
ρ_p	*The density of solid phase (kg/m^3)*
v_g	*The gas flow velocity (m/s)*
v_p	*The motion velocity of particle (m/s)*
p	*The gas phase pressure (Pa)*
τ_g	*The gas stress tensor*
ϕ_g	*The gas volume fraction*
f_{dr}	*The average fluid resistance of the particle in control body (N)*
∇V	*The respectively represent the volume of calculated control body*
V_i	*The volume of particle i in the midst of the control body (m^3)*
l	*he number of particle in the control body*

e	*The restitution coefficient of particle*
$\vec{n}$	*The unit vector from the center of particle 1 point to the contact point*
m	*The particle mass (kg);* R *is the particle radius (m)*
ω	*The angular velocity of particle (rad/s)*
$\overrightarrow{G^0}$	*The relative velocity before collision of the contact point (m/s)*
$\overrightarrow{G_{ct}^0}$	*The tangential component of the relative velocity before collision (m/s)*
$\vec{t}$	*The unit tangential vector on contact point*
d_p	*The radius of solid phase (m)*
C_D	*The drag coefficient*
g	*The gravity acceleration (m/s^2)*
g_z	*The acceleration of gravity on direction Z (m/s^2)*
F_z	*The other force on direction Z, including additional Mass Force, Thermophoretic Force, Brownian Force and Saffman Lift Force*
E	*The surface erosion rate (kg/m^2.s)*
γ	*The collision angle between the particle path and throttle surface (°)*
R_T	*The tangential recovery ratio*
γ_0	*The maximum erosion angle (°)*
k_2	*1*
k_{12}	*constant*
v_1, v_2, v_3	*The relative velocities (m/s)*

References

[1] Wang RH, Zang YB, Zhang R, *et al.* Drillstring failure analysis and its prevention in northeast Sichuan, China. Engineering Failure Analysis 2011; 18: 1233-1241.

[2] Molaleye B. A review of light amplification by stimulated emission of radiation in oil and gas well drilling. Mining Science and Technology (China) 2010; 20: 752-757.

[3] Fan YT, Huang ZQ, Gao DL, Li Q. Experimental study of an Al_2O_3/WC–Co nano-composite based on a failure analysis of hammer bit. Engineering Failure Analysis 2011; 18: 1351-1358.

[4] Finnie I. Erosion of surfaces by solid particles. Wear 1960; 3: 87-103.

[5] Humphrey JAC. Fundamentals of fluid motion in erosion by solid particle impact. International Journal of Heat and Fluid Flow 1990; 11: 170-195.

[6] McLaury BS, Wang J, Shirazi SA, et al. Solid particle erosion in long radius elbows and straight pipes. Presented at 1997 SPE Annual Technical Conference and Exhibition, San Antonio, SPE paper No.:38842.

[7] Liebhard M, Levy A. The effect of erodent particle characteristics on the erosion of metals. Wear 1991; 151: 381-390.

[8] Nojabaei B, Mansoori Z, Saffar-Avval M. Heat transfer in turbulent liquid-solid flow considering the interparticlecollision effect. Petroleum Science and Technology 2012; 30: 1296-1306.

[9] Habib MA, Badr HM, Ben-Mansour R, et al. Numerical calculations of erosion in an abrupt pipe contraction of different contraction ratios. International Journal for Numerical Methods in Fluids 2004; 46: 19-35.

[10] Arefi B, Settari A, Angman P. Simulation of erosion in drilling tools for the oil and gas industry. Journal of Canadian Petroleum Technology 2006; 45: 34-40.

[11] Zhu HJ, Lin YH, Zeng DZ, et al. Numerical analysis of flow erosion on drill pipe in gas drilling. Engineering Failure Analysis 2012; 22: 83-91.

[12] Zhang YL. Application and improvement of computational fluid dynamics (CFD) in solid particle erosion modeling. The University of Tulsa 2006.

[13] Oka Y, Okamura K, Yoshida T. Practical estimation of erosion damage caused by solid particle impact, Part 1: Effects of impact parameters on a predictive equation. Wear 2005; 259: 95-101.
[14] Mazumder QH, Siamack AS, Mclaury BS. Prediction of solid particle erosive wear of elbows in multiphase annular flow-model development and experiment validations. Journal of Energy Resources Technology 2008; 130: 1-10.
[15] Oka Y, Yoshida T. Practical estimation of erosion damage caused by solid particle impact, Part 2: Mechanical properties of materials directly associated with erosion damage. Wear 2005; 259: 102-109.
[16] Liu CB, Jiang SL, Zheng YG. Experimental and computational failure analysis of a valve in a nuclear power plant. Engineering Failure Analysis 2012; 22: 1-10.
[17] Ali SF, Yeung H. Experimental investigation and numerical simulation of two-phase flow in a large-diameter horizontal flow line vertical riser. Petroleum Science and Technology 2010; 28: 1079-1095.